

Electron- and neutrino-nucleus scattering

Omar Benhar

INFN and Department of Physics, Università “La Sapienza”
Piazzale Aldo Moro, 2. I-00185 Roma, Italy

I review the main features of the nuclear response extracted from electron scattering data. The emerging picture clearly shows that the shell model does not provide a fully quantitative description of nuclear dynamics. On the other hand, many body approaches in which correlation effects are explicitly taken into account lead to a satisfactory account of electron scattering observables. The possibility of exploiting the knowledge acquired from electron scattering to reduce the systematic uncertainty of neutrino oscillation experiments is outlined.

1. Introduction

Over the past four decades electron scattering has provided a wealth of information on nuclear structure and dynamics. Form factors and charge distributions have been extracted from elastic scattering data, while inelastic measurements have allowed for a systematic study of the dynamic response over a broad range of momentum and energy transfer. Finally, with the advent of the last generation of continuous beam accelerators, a number of exclusive processes have been analyzed with unprecedented precision. Recent theoretical and experimental developments in the field of electron-nucleus scattering are reviewed in Ref. [1].

In electron scattering experiments the nucleus is mostly seen as a target. Studying its interactions with the probe, whose properties are completely specified, one obtains information on the unknown features of its internal structure. In neutrino oscillation experiments, on the other hand, nuclear interactions are exploited to detect the beam particles, whose kinematics is largely unknown.

Using the nucleus as a detector obviously requires that its response to neutrino interactions be under control at a quantitative level. Fulfillment of this prerequisite is in fact critical to keep the systematic uncertainty associated with the reconstruction of the neutrino kinematics to an acceptable level.

This paper is aimed at providing a summary of the picture of the nuclear response emerging from the analysis of electron-nucleus scattering data, and suggesting a possible strategy to exploit the knowledge acquired from electron scattering in the analysis of the next generation of high precision neutrino experiments.

In Section 2 I will briefly review the experimental evidence pointing to the inadequacy of the mean field picture of nuclear dynamics and discuss the role of nucleon-nucleon (NN) correlations. Section 3 is devoted to an overview of nonrelativistic nuclear many body theory and its applications to electron scattering observables. In Section 4 I will outline the possible implementation of a state of the art theoretical description of the nuclear response in the analysis of neutrino oscillation experiments. Finally, the conclusions are stated in Section 5.

2. Splendor and miseries of the nuclear shell model

The nuclear shell model is based on the assumption that nucleons in a nucleus behave as independent particles moving in a mean field. Within this picture the many body Schrödinger equation reduces to a single particle problem, whose solution yields the energies and wave functions associated with the one-nucleon states. For example, the shell model ground state of oxygen consists of a core of four nucleons in S -states, i.e.

carrying orbital angular momentum $\ell = 0$, and twelve nucleons in the valence P -states, i.e. with $\ell = 1$. Higher energy levels are not occupied.

Electron scattering experiments aimed at assessing the limits of applicability of the nuclear shell model, pioneered by the Frascati group in the mid sixties [2] and systematically pursued in several laboratories over the past four decades (reviews of $(e, e'p)$ experiments can be found in, e.g., Refs. [1,3]), are mainly based on measurements of the cross section of the proton knock out process

$$e + A \rightarrow e' + p + (A - 1) . \quad (1)$$

The most striking feature emerging from the analysis of $(e, e'p)$ data is that, while the spectroscopic lines corresponding to knock out from shell model states are clearly seen, the corresponding strengths are consistently and sizably lower than expected, regardless of the nuclear mass number.

Fig. 1 shows a recent compilation of the strengths of the valence shell model orbits of a number of nuclei, ranging from carbon to lead, measured by both electron- and hadron-induced proton knock out [4]. It clearly appears that all the observed strengths are largely below the shell model prediction.

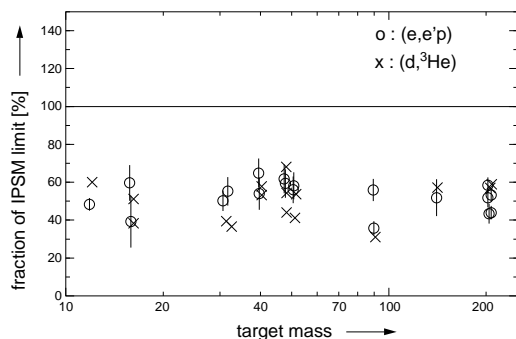


Figure 1. Integrated strengths of the valence shell model states, measured in electron- (open circles) and hadron-induced (crosses) proton knock out experiments, as a function of the target mass number (taken from Ref. [4]). The solid horizontal line represents the shell model prediction.

The data displayed in Fig. 1 demonstrate that

a significant fraction of the target nucleons *do not* behave as independent particles, thus providing one of the cleanest signatures of correlation effects. Strong NN interactions give rise to virtual scattering processes leading to the excitation of the participating nucleons to states of energy larger than the Fermi energy, thus depleting the shell model states within the Fermi sea.

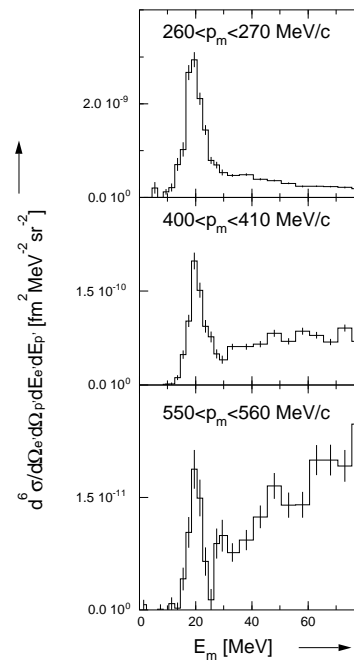


Figure 2. Proton removal energy spectra measured in $(e, e'p)$ processes off ${}^4\text{He}$ [6]. The different panels correspond to different proton momentum ranges.

To estimate the typical energy scale associated with NN correlations, consider a pair of correlated nucleons, carrying momenta \mathbf{p}_1 and \mathbf{p}_2 much larger than the Fermi momentum (~ 200 MeV). In the nucleus rest frame, as all the remaining $A - 2$ particles carry low momenta, $\mathbf{p}_1 \approx -\mathbf{p}_2 = \mathbf{p}$. Hence, knock out of a nucleon of large momentum \mathbf{p} leaves the residual system with a particle in the continuum and requires an energy

$$E \approx E_{thr} + \frac{\mathbf{p}^2}{2m} , \quad (2)$$

much larger than the Fermi energy (~ 30 MeV). The above equation, where E_{thr} denotes the threshold for two-nucleon removal, shows that large separation energy and large nucleon momentum are strongly correlated.

Coincidence ($e, e'p$) experiments have confirmed the validity of the simple argument leading to Eq.(2). Measurements carried out using ${}^3\text{He}$ and ${}^4\text{He}$ targets have clearly shown that, while the knock out of a low momentum proton yields an energy spectrum featuring a sharp peak corresponding to the transition to a bound state of the residual system, the spectra associated with knock out of high momentum nucleons exhibit a broad bump, whose maximum is located at an energy roughly given by Eq.(2) [5,6]. These features are clearly visible in the data shown in Fig. 2

A systematic study of proton knock out extending to momenta ~ 700 MeV and energy ~ 200 MeV has been recently completed at Jefferson Lab using carbon, iron and gold targets. Although the data is still being analyzed, the available results appear to confirm the presence of an amount of correlated strength consistent with the observed depletion of the shell model states [7,8].

3. Many body theory of electron-nucleus scattering

Within the impulse approximation (IA) scheme, which is expected to be applicable at large momentum transfer, electron-nucleus scattering is described as an incoherent sum of elementary scattering processes involving only one nucleon, the remaining $A - 1$ particle acting as spectators. It follows that, neglecting final state interactions (FSI) between the struck proton and the residual system, the cross section of process (1) can be written in a simple factorized form, generally referred to as plane wave impulse approximation (PWIA)

$$\frac{d\sigma_{PWIA}}{d\omega d\Omega_{e'} d\Omega_{p'} dT_{p'}} = |\mathbf{p}'|(m+T_{p'})\sigma_{ep}P(\mathbf{p}_m, E_m). \quad (3)$$

In the above equation m and \mathbf{p}' and $T_{p'}$ denote the proton mass, momentum and kinetic energy, respectively, while the missing momentum \mathbf{p}_m and missing energy E_m are defined as $\mathbf{p}_m = \mathbf{p}' - \mathbf{q}$

and $E_m = \omega - T_{p'} - T_R$, \mathbf{q} , ω and T_R being the momentum end energy transfer and the kinetic energy of the recoiling spectator system.

The electron-proton scattering process is described by the elementary cross section σ_{ep} , while all the information on nuclear dynamics is contained in the spectral function $P(\mathbf{p}, E)$, defined as (see, e.g., ref.[9])

$$P(\mathbf{p}, E) = \sum_n \left| \langle \Psi_n^{(A-1)} | a_{\mathbf{p}} | \Psi_0^A \rangle \right|^2 \times \delta(E + E_0 - E_n). \quad (4)$$

In the above equation, $|\Psi_0^A\rangle$ and $|\Psi_n^{(A-1)}\rangle$ describe the target ground state and the final state of the spectator system, respectively, while E_0 and E_n are the corresponding energies. The spectral function yields the probability of removing a nucleon carrying momentum \mathbf{p} from the target ground state leaving the residual system with energy E .

Nuclear many body theory (NMBT) provides a fully consistent computational framework to obtain the spectral function of Eq.(4). Within this approach the nucleus is viewed as a collection of pointlike protons and neutrons, whose dynamics is described by the nonrelativistic hamiltonian

$$H = \sum_i \frac{\mathbf{p}_i^2}{2m} + \sum_{j>i} v_{ij} + \sum_{k>j>i} V_{ijk}. \quad (5)$$

The two body potential v_{ij} is determined by fitting deuteron properties and nucleon-nucleon scattering data, while inclusion of the three-nucleon interaction is needed to reproduce the binding energy of the three-nucleon systems.

The many body Schrödinger equation associated with the hamiltonian of Eq.(5) can be solved exactly, using stochastic methods, for nuclei with mass number up to 10. The resulting energies of the ground and low-lying excited states are in excellent agreement with experimental data [10]. Accurate calculations can also be carried out for uniform nuclear matter [11].

The spectral functions obtained within NMBT have been extensively used in the analysis of a variety of electron scattering observables (for a review see, e.g., ref.[12]). As an example, Fig. 3 shows the comparison between the strengths

of the shell model states of ^{208}Pb measured at NIKHEF [13] and the theoretical results of ref.[14]. It clearly appears that the energy dependence of the depletion due to NN correlations is understood at a quantitative level.

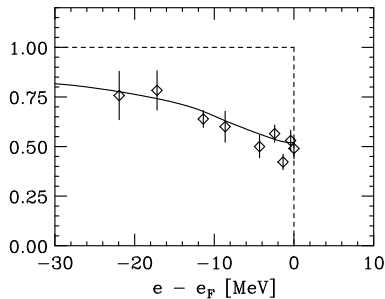


Figure 3. Strengths of the single particle states of ^{208}Pb measured at NIKHEF, plotted as a function of the difference between their energies and the Fermi energy [13]. The solid line shows the results of the theoretical calculation of ref.[14], based on NMBT, while the dashed horizontal line corresponds to the shell model prediction.

The effect of FSI, neglected to obtain Eq.(3), has long been recognized to be sizable. Over the past decade a series of measurements of the nuclear transparency to protons knocked out in $(e, e'p)$ processes, carried out at MIT Bates [15], SLAC [16] and Jefferson Lab [17,18] have consistently shown deviations of more than 50 % from the PWIA limit.

Within NMBT FSI effects can be included using the same dynamics employed to describe the initial state. In the approach developed in ref. [19] the motion of the knocked out nucleon is treated within the eikonal approximation while the spectators are seen as a collection of fixed scattering centers. Applications to the analysis of inclusive data in the region of very low energy transfer, which is known to be dominated by FSI effects, have been quite successful [19,20,21].

Fig. 4 shows the Q^2 -dependence of the transparency ratio

$$T_A(Q^2) = \frac{d\sigma_{expt}}{d\sigma_{PWIA}}, \quad (6)$$

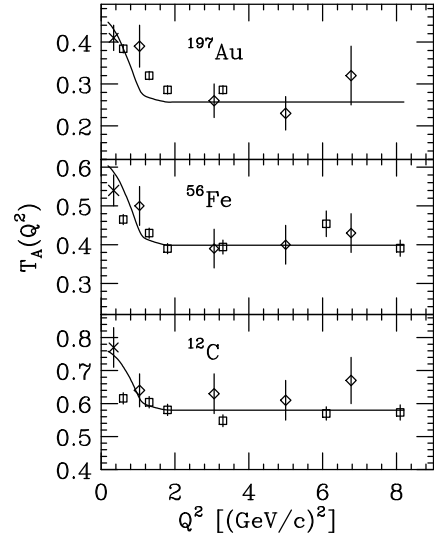


Figure 4. Q^2 -dependence of the transparencies of carbon, iron and gold calculated using the local density approximation (LDA) and the approach of ref.[19]. The data points are from refs.[15] (crosses), [16] (diamonds) and [17,18] (squares).

whose numerator is the observed cross section, whereas the denominator is the PWIA cross section of Eq.(3). From the above definition it follows that in absence of FSI $T_A(Q^2) \equiv 1$.

The theoretical results have been obtained using the approach of ref. [19], whose main ingredients are the measured NN scattering amplitude, corrected to take into account medium modifications [22], and the space distribution of the spectator particles, calculated within the local density approximation (LDA).

It has to be pointed out that the probability of rescattering in the final state does not simply depend upon the nuclear density distribution, yielding the probability of finding a spectator at position \mathbf{r}_s , but upon the *joint* probability of finding the struck particle at position \mathbf{r} and a spectator at position \mathbf{r}_s . Due to the strongly repulsive nature of NN interactions at short range this quantity is strongly affected by NN correlations, whose inclusion leads to a sizable enhancement of the transparency. For example, in lead correlation produce a $\sim 20\%$ effect on $T_A(Q^2)$.

4. Implementing many body theory in the analysis of neutrino experiments

In the analysis of neutrino experiments nuclear effects are mostly described using the ultimate independent particle model: the Fermi gas (FG) model [23], according to which the nucleus can be approximated by a degenerate gas of protons and neutrons.

The results of the previous Sections, showing that independent particle models fail to provide a quantitative account of the nuclear electromagnetic response, strongly suggest that correlation effects be large, and must therefore be taken into account in the analysis of high precision neutrino oscillation experiments. To see this, consider, for example, the quasielastic charged-current process

$$\nu + A \rightarrow \ell + p + (A - 1) . \quad (7)$$

Neutrino kinematics is dictated by energy and momentum conservation, requiring

$$E_\nu + M_A = E_\ell + E_{p'} + E_{A-1} , \quad (8)$$

M_A being the nuclear mass, and

$$\mathbf{p}_\nu = \mathbf{p}_\ell + \mathbf{p}' + \mathbf{p}_{A-1} , \quad (9)$$

where \mathbf{p}' denotes the momentum of the outgoing proton,

$$E_{p'} = \sqrt{\mathbf{p}'^2 + m^2} \quad (10)$$

and

$$E_{A-1} = \sqrt{\mathbf{p}_{A-1}^2 + (M_A - m + E)} , \quad (11)$$

E being the removal energy of the struck nucleon carrying initial momentum $\mathbf{p} \sim -\mathbf{p}_{A-1}$.

In the FG model all nucleon momenta are lower than the Fermi momentum $p_F \sim 200$ MeV, while typical removal energies are in the range $\sim 25-35$ MeV [24]. On the other hand, realistic spectral functions, on account of NN correlations pushing strength to high momentum *and* high energy (see Eq.(2)), yield [9,21]

$$\langle E \rangle = \int d^3p dE P(\mathbf{p}, E) \sim 40 - 65 \text{ MeV} , \quad (12)$$

leading to a neutrino energy sizably different from that obtained using the FG model.

The discussion of Section 2 also suggest that the FG model be inadequate to describe the final state. Strong dynamical NN correlations, leading to large density fluctuations over a length scale of ~ 1 fm, have been shown to sizably affect the probability of rescattering of the hadrons produced at the weak interaction vertex.

In spite of its success in explaining electron-scattering data, it has to be realized that exploitation of NMBT in the analysis of neutrino oscillation experiments, in which the nucleus is seen as a detector rather than a target, largely depends upon the possibility of implementing the theoretical knowledge in Monte Carlo simulations.

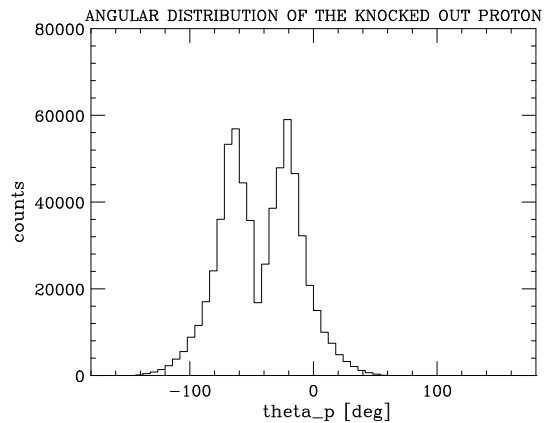


Figure 5. Angular distribution of the knocked out proton obtained from a Monte Carlo simulation of the process $(e, e'p)$ off oxygen at beam energy 700 MeV, energy of the scattered electron 500 MeV and electron scattering angle 30° . The kinetic energy of the outgoing proton is in the range 160 - 180 MeV.

Assuming, for the sake of simplicity, that the elementary weak interaction vertex in the nuclear medium be the same as in free space, a realistic simulation of neutrino-nucleus scattering requires the energy and momentum probability distribution of the nucleons, their distribution in space and the medium modified hadronic cross section needed for the description of FSI.

NMBT provides a *parameter free* approach that allows one to calculate all the above quantities in a fully consistent fashion.

As an example, Fig. 5 shows the proton angular distribution resulting from a simulation of the $(e, e'p)$ reaction off oxygen. The calculations have been carried out using a spectral function obtained within the LDA [25], ground state configurations sampled from the probability distribution associated with the wave function of ref.[26] and the medium modified NN differential cross sections of ref.[22]. The spectrum of Fig. 5 corresponds to beam energy $E_e = 700$ MeV, energy of the scattered electron $E'_e = 500$ MeV and electron scattering angle $\theta_e = 30^\circ$. The kinetic energy of the outgoing proton is in the range 160–180 MeV.

Thanks to the steady progress of the stochastic techniques to solve the many body Schrödinger equation, the ingredients needed to carry out realistic simulations for targets other than oxygen are expected to become available within the next few years.

5. Conclusions

The results discussed in this paper show that electron scattering experiments have exposed the deficiencies of the independent particle model of nuclear dynamics. On the other hand, many body approaches explicitly including dynamical correlation effects provide a quantitative account of a number of electron scattering observables, and appear to be a computationally viable option to improve the treatment of nuclear effects in the analysis of neutrino oscillations experiments.

Acknowledgments

The author is indebted to V.R. Pandharipande, M. Sakuda, R. Seki and I. Sick for many illuminating discussions.

REFERENCES

1. *Electron Nucleus Scattering VII*, Eds. O. Benhar, A. Fabrocini, S. Fantoni and R. Schiavilla, Eur. Phys. J. A **17** (2003).
2. U. Amaldi Jr., *et al*, Phys. Rev. Lett. **13** (1964) 341.
3. *Modern Topics in Electron Scattering*, Eds. B. Frois and I. Sick (World Scientific, Singapore, 1991).
4. G.J. Kramer, H.P. Block and L. Lapikas, Nucl. Phys. **A679** (2001) 267
5. C. Marchand, *et al*, Phys. Rev. Lett. **60** (1984) 1703.
6. J.J. Van Leeuwe, *et al*, Nucl. Phys. **A631** (1998) 593c.
7. D. Rohe, Eur. Phys. J. A **17** (2003) 439.
8. D. Rohe, *et al*, nucl-ex/0405028. Submitted to Phys. Rev. Lett.
9. O. Benhar, A. Fabrocini and S. Fantoni, Nucl. Phys. **A505** (1989) 267.
10. S.C. Pieper and R.B. Wiringa, Ann. Rev. Nucl. Part. Sci. **51** (2001) 53.
11. A. Akmal, V. R. Pandharipande, Phys. Rev. C **56** (1997) 2261.
12. O. Benhar, V.R. Pandharipande and S.C. Pieper, Rev. Mod. Phys. **65** (1993) 817.
13. E.N.M. Quint, Ph. D. Thesis, University of Amsterdam (1998).
14. O. Benhar, A. Fabrocini and S. Fantoni, Phys. Rev. C **41** (1990) R24.
15. G. Garino *et al*, Phys. Rev. C **45** (1992) 78.
16. T.G. O'Neill *et al*, Phys. Lett. **B351** (1995) 87.
17. D. Abbott *et al*, Phys. Rev. Lett. **80** (1998) 5072.
18. K. Garrow *et al*, Phys. Rev. C **66** (2002) 044613.
19. O. Benhar *et al*, Phys. Rev. C **44** (1991) 2328.
20. O. Benhar and V.R. Pandharipande, Phys. Rev. C **47** (1993) 2218.
21. O. Benhar, A. Fabrocini, S. Fantoni and I. Sick, Nucl. Phys. **A579** (1994) 493.
22. V.R. Pandharipande and S.C. Pieper, Phys. Rev. C **45** (1992) 791.
23. E.J. Moniz, Phys. Rev. **184** (1969) 1154.
24. E.J. Moniz *et al*, Phys. Rev. Lett. **26** (1971) 445.
25. O. Benhar, nucl-th/0307061, to be published in the Proceedings of NUINT02 (Nucl. Phys. B, Proc. Suppl.).
26. S.C. Pieper, R.B. Wiringa and V.R. Pandharipande, Phys. Rev. C **46** (1992) 1741.